**<Supporting Information>**

# Utilizing the adaptive precursor $[As_2W_{19}O_{67}(H_2O)]^{14-}$ to support three hexanuclear lanthanoid-based polytungstoarsenate dimers

Huafeng Li,[a] Hechen Wu,[a] Rong Wan,[a] Yuan Wang,[a] Pengtao Ma,[a] Suzhi Li,[b] Jingping Wang[a]* and Jingyang Niu[a]*

[a] *Henan Key Laboratory of Polyoxometalate Chemistry, College of Chemistry and Chemical Engineering, Henan University, Kaifeng, Henan 475004, China*

[b] *College of Chemistry and Chemical Engineering, Engineering Research Center of Functional Material Preparation, Shangqiu Normal University, Shangqiu, 476000, Henan, China*

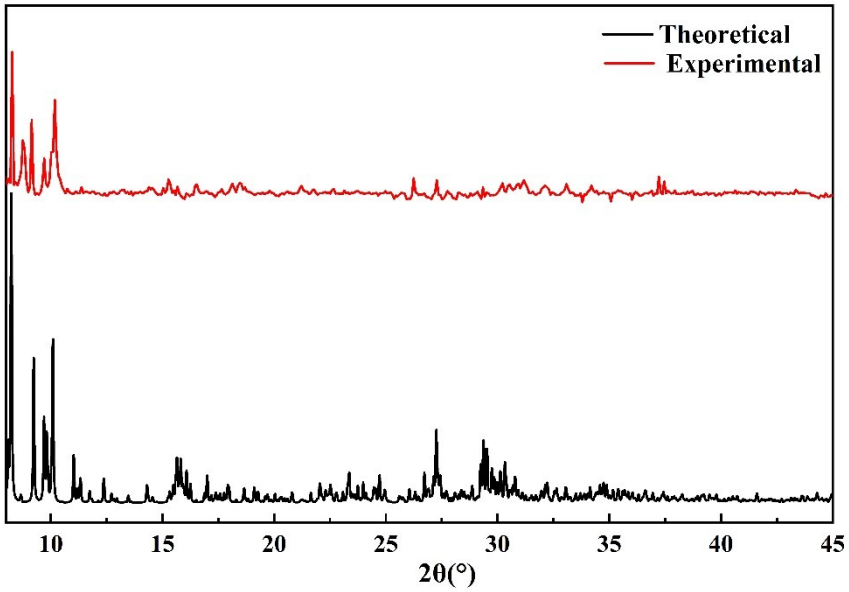


**Figure S1.** The X-ray powder diffraction patterns of **1Eu**.

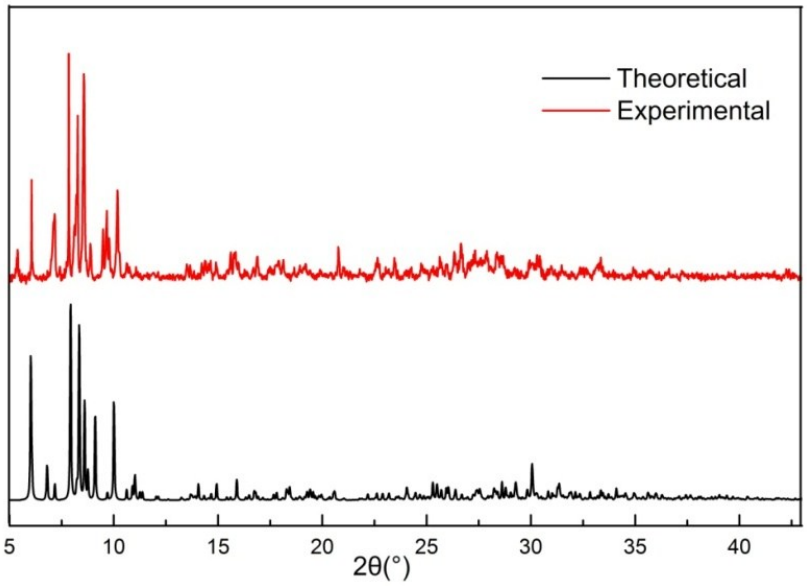


**Figure S2.** The X-ray powder diffraction patterns of **2Tb**.

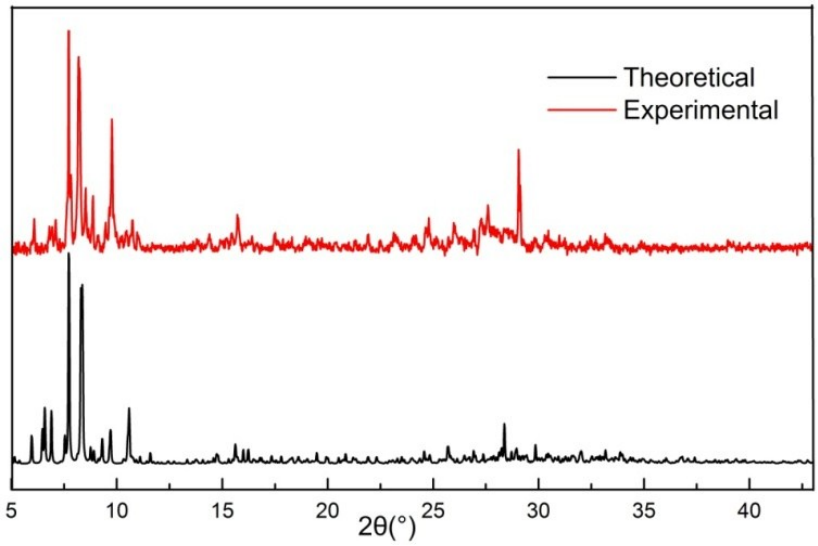


**Figure S3.** The X-ray powder diffraction patterns of **3Dy**.

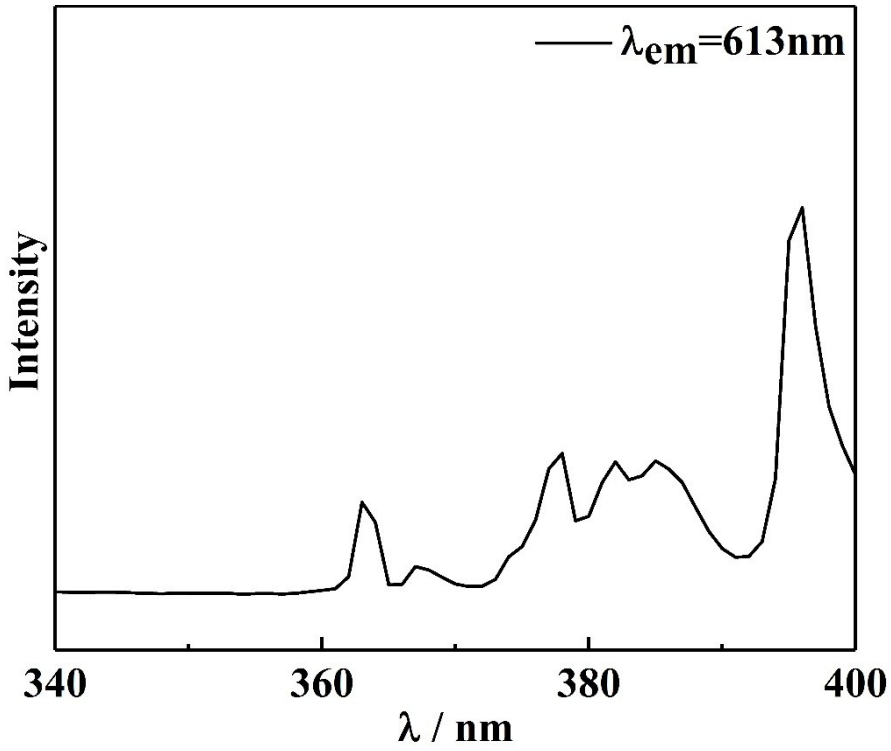


**Figure S4.**The excitation spectrum of **1Eu** in the solid state at room temperature.

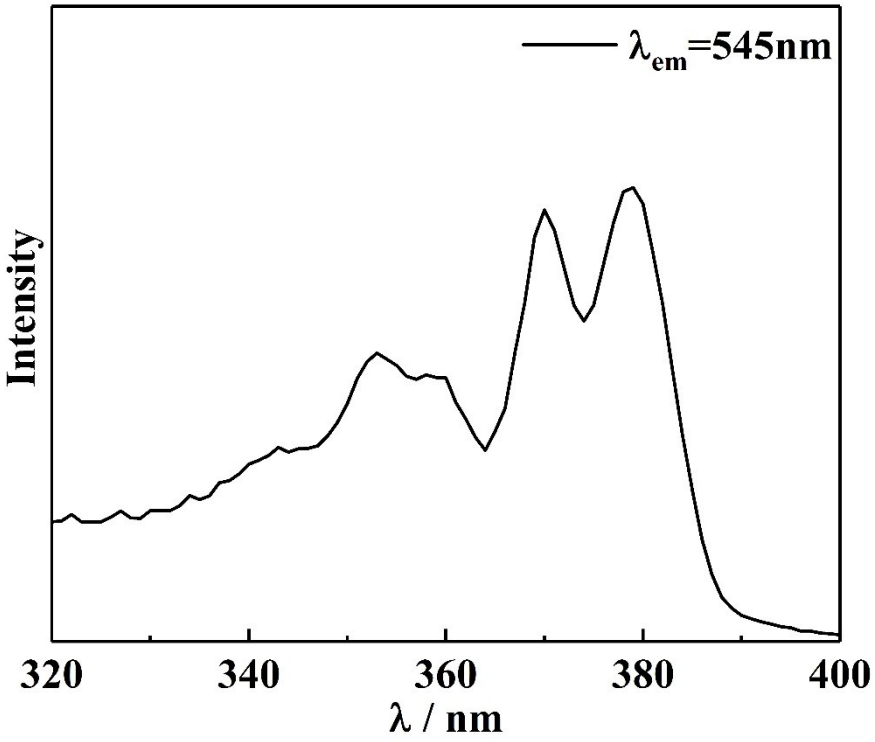


**Figure S5.** The excitation spectrum of **2Tb** in the solid state at room temperature.

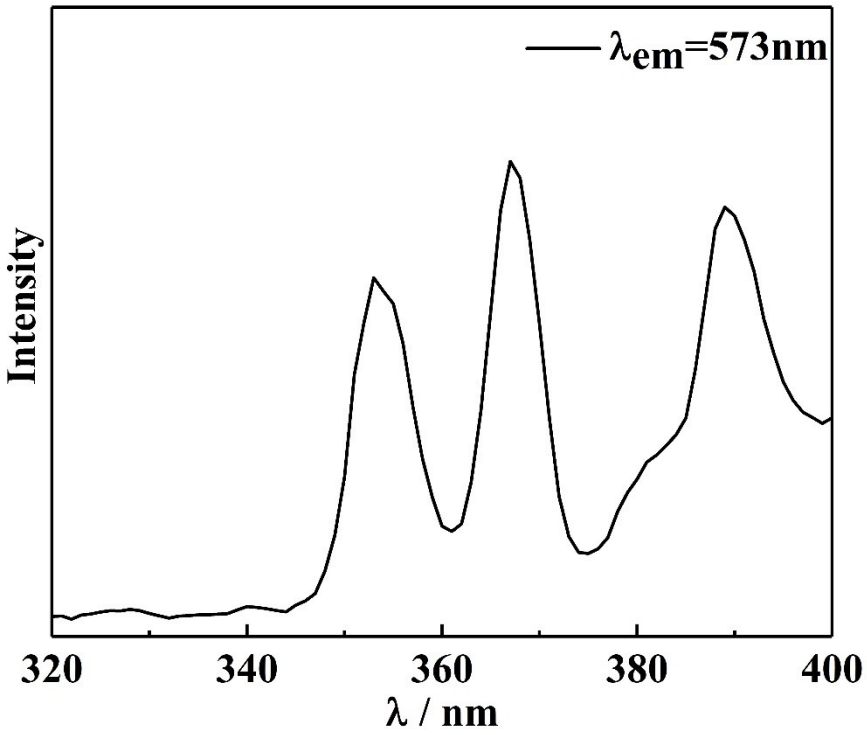


**Figure S6.** The excitation spectrum of **3Dy** in the solid state at room temperature.

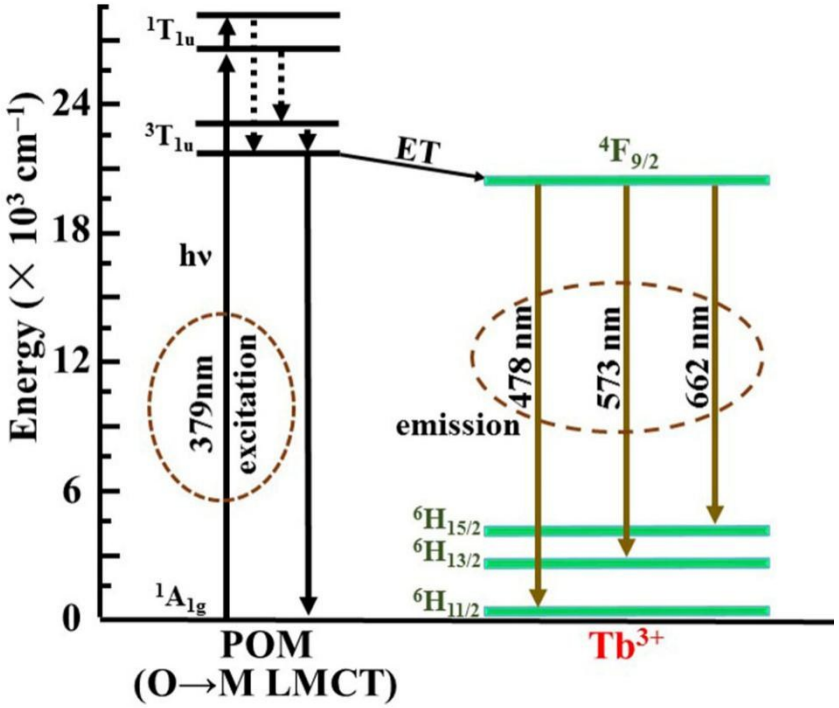


**Figure S7.** The schematic energy level diagram demonstrating energy transfer process from POM to $Tb^{3+}$ ions and characteristic emissions of $Tb^{3+}$ ions (dotted line denotes nonradiative transition).

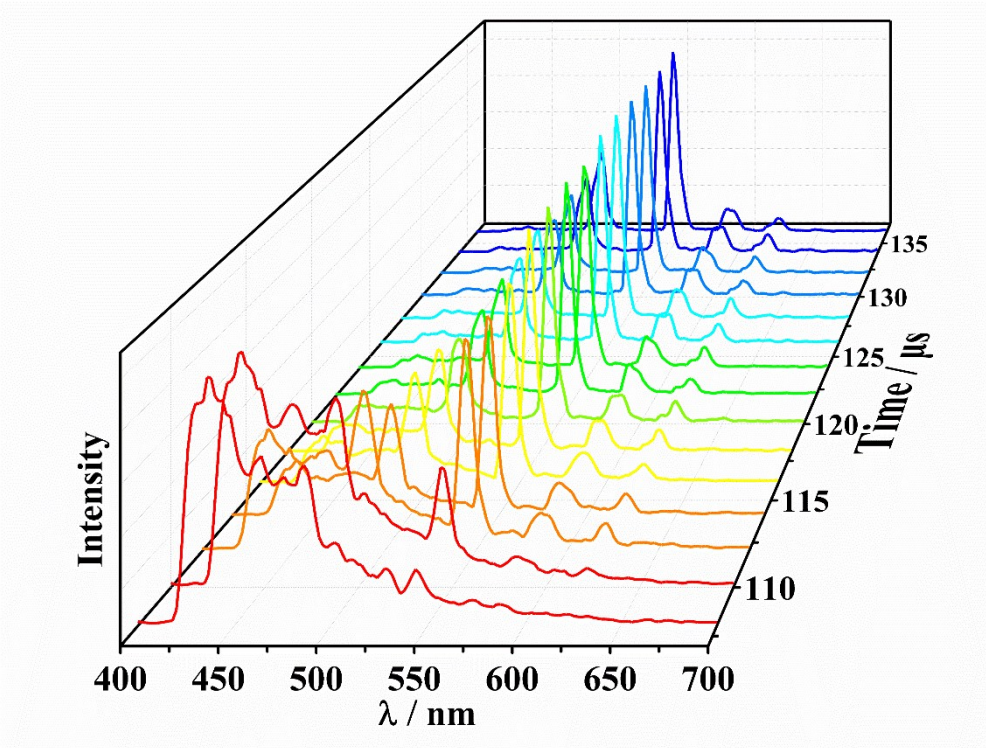


**Figure S8.** The time-resolved emission spectroscopy of **2Tb** powder sample under excitation wavelength at 379 nm.

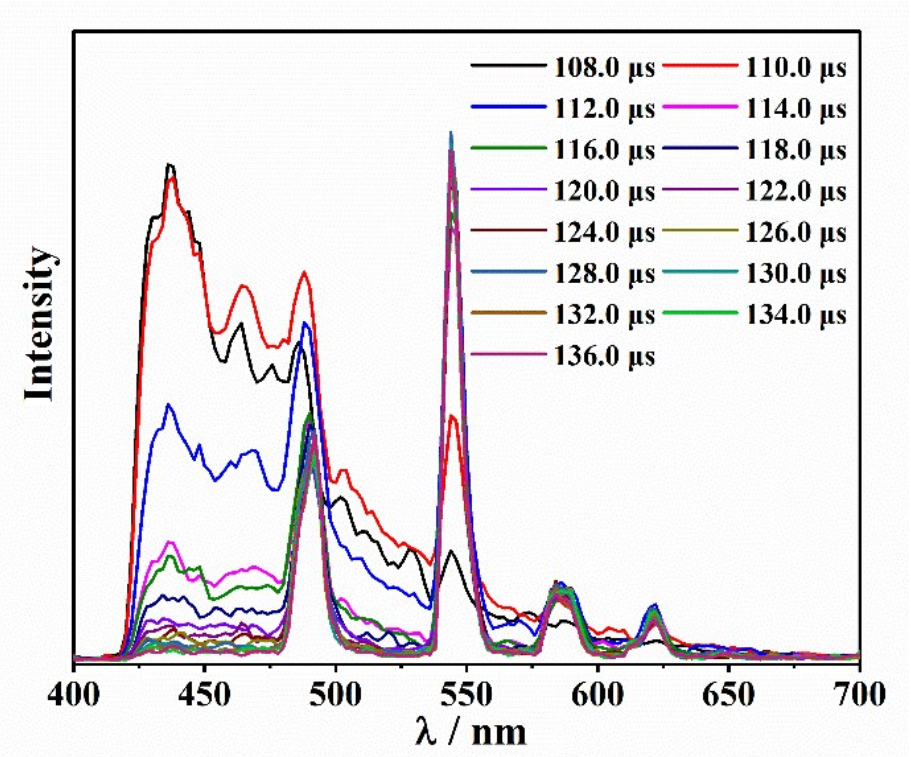


**Figure S9.** Spectral temporal evolution of **2Tb**.

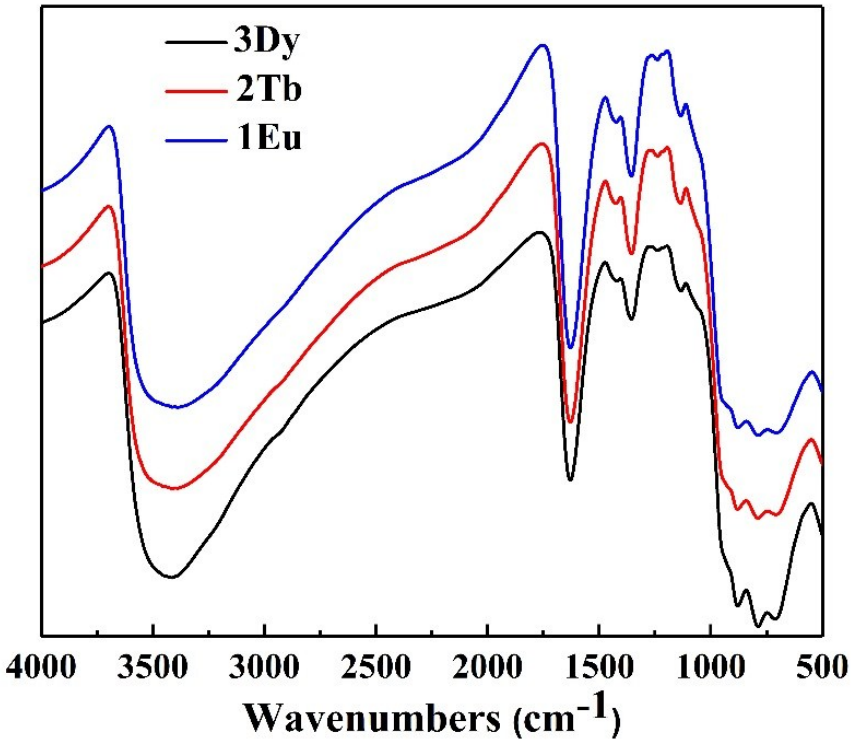


**Figure S10.** IR spectra of **1Eu–3Dy**.

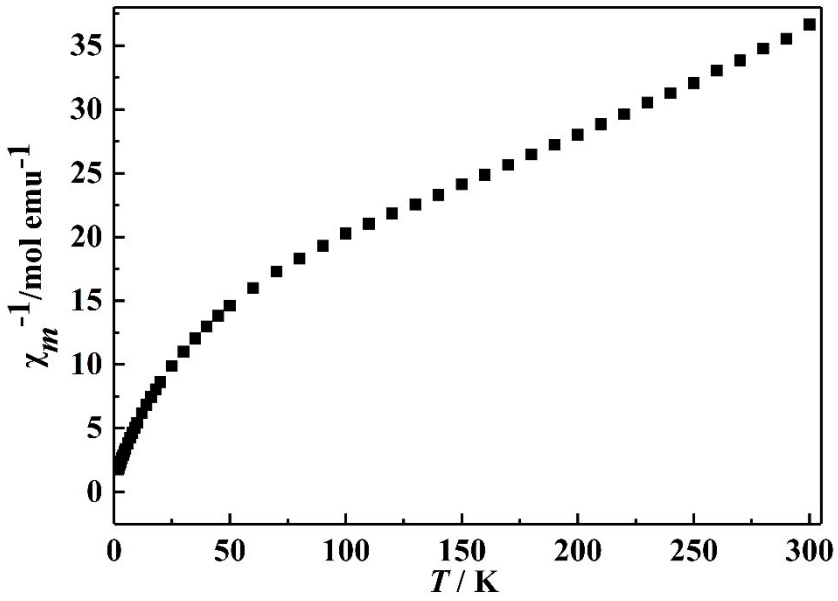


**Figure S11.** $\chi_m^{-1}$ *vs T* curve of **1Eu**.

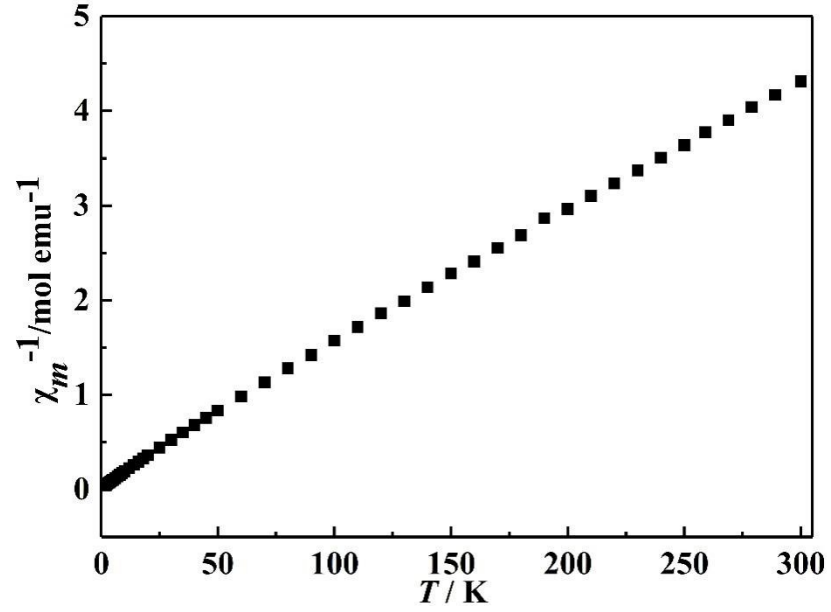


**Figure S12.** $\chi_m^{-1}$ *vs T* curve of **2Tb**.

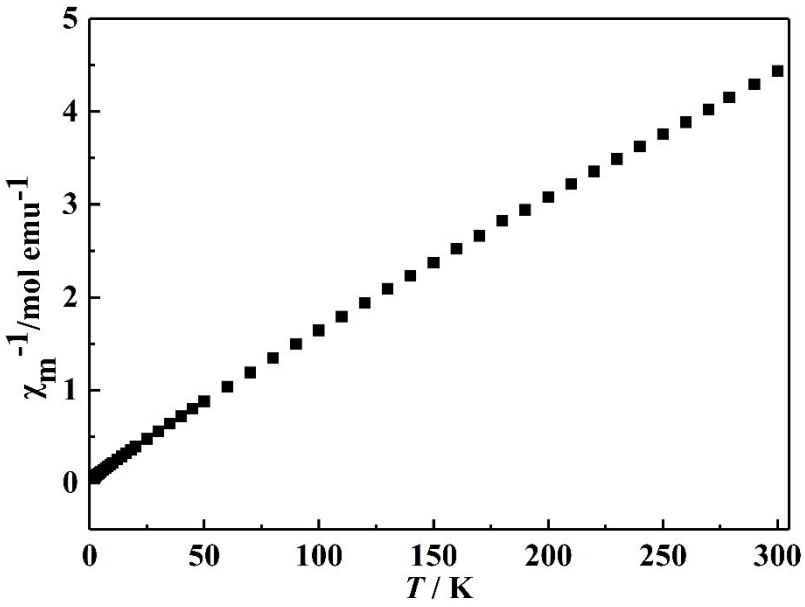


**Figure S13.** $\chi_m^{-1}$ *vs T* curve of **3Dy**.

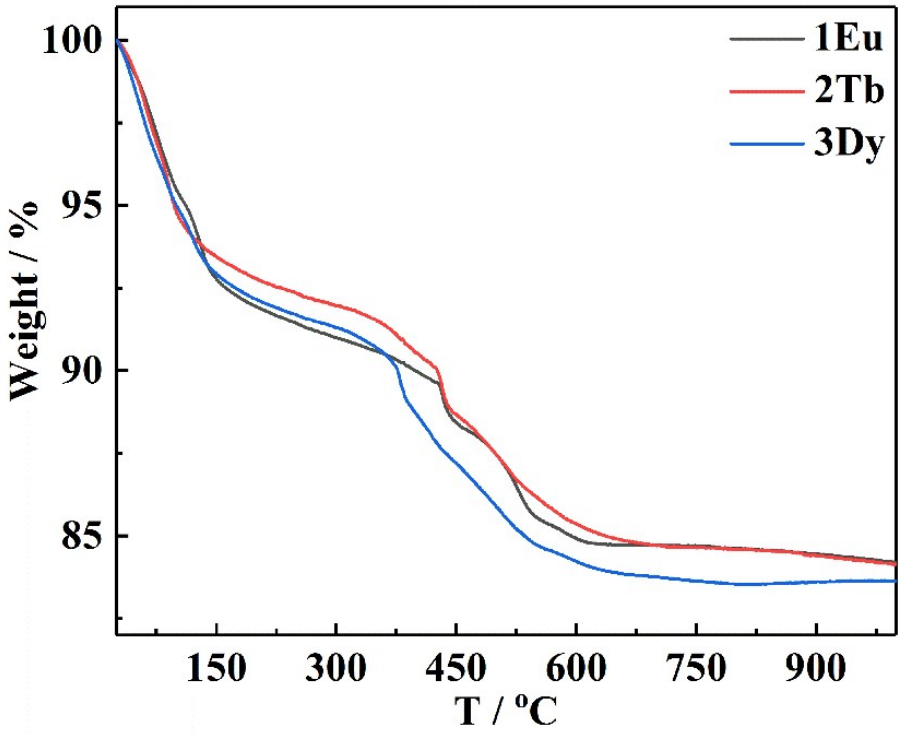


**Figure S14.** The thermogravimetric curves of **1Eu–3Dy**.

**Table S1.** BVS values of As, W and Eu atoms of compound **1Eu**.

| Atom | BVS | Atom | BVS | Atom | BVS | Atom | BVS |
|---|---|---|---|---|---|---|---|
| As1 | 3.05 | W2 | 6.23 | W8 | 6.23 | W14 | 6.05 |
| As2 | 3.11 | W3 | 6.34 | W9 | 6.04 | W15 | 6.43 |
| Eu1 | 3.34 | W4 | 6.16 | W10 | 6.30 | W16 | 6.24 |
| Eu2 | 3.04 | W5 | 6.32 | W11 | 6.06 | W17 | 6.39 |
| Eu3 | 3.30 | W6 | 6.10 | W12 | 6.38 | W18 | 6.15 |
| W1 | 6.31 | W7 | 6.00 | W13 | 6.14 | W19 | 6.39 |

**Table S2.** BVS values of selected oxygens atoms in **1Eu**-**3Dy**.

| BVS | | | | | | | | protonation |
|---|---|---|---|---|---|---|---|---|
| **1Eu** | | **2Tb** | | **3Dy** | | | | |
| O1W | −0.39 | O1W | −0.38 | O1W | −0.34 | O9W | −0.34 | diprotonated |
| O2W | −0.35 | O2W | −0.34 | O2W | −0.30 | O10W | −0.30 | diprotonated |
| O3W | −0.39 | O3W | −0.33 | O3W | −0.30 | O11W | −0.31 | diprotonated |
| O4W | −0.37 | O4W | −0.32 | O4W | −0.35 | O12W | −0.36 | diprotonated |
| O5W | −0.36 | O5W | −0.37 | O5W | −0.33 | O13W | −0.29 | diprotonated |
| O6W | −0.34 | O6W | −0.32 | O6W | −0.34 | O14W | −0.37 | diprotonated |
| O7W | −0.36 | O7W | −0.35 | O7W | −0.34 | O151 | −0.54 | diprotonated |
| O42 | −0.59 | O42 | −0.60 | O8W | −0.34 | | | diprotonated |
| O39 | −0.98 | O39 | −0.91 | O146 | −0.90 | | | monoprotonated |
| O43 | −1.14 | O43 | −1.09 | O149 | −0.99 | | | monoprotonated |

**Table S3.** The thermogravimetric analyses of compound **2Tb** and compound **3Dy**.

| Compound | Theoretical (two steps, %) | Experimental (two steps, %) |
|---|---|---|
| **1Eu** | 8.47, 6.57 | 8.90, 6.61 |
| **2Tb** | 6.23, 4.25 | 6.81, 4.77 |
| **3Dy** | 6.28, 6.10 | 8.42, 7.04 |

**Thermogravimetric Analyses.**

As shown in Figure S14, the thermal stability of compounds **1Eu**–**3Dy** have been determined by using thermogravimetric analyses. The thermogravimetric curves are very similar and show two major weight loss stages in the region of 25–1000 ºC. Hence, only the thermogravimetric curve of **1Eu** is taken as a representative to describe in detail. For **1Eu**, the observed total weight loss (15.51 %) is agreement with the calculated value (15.04 %). The first weight loss of 8.90 % from 25 to 425 ºC was due to the release of fifty lattice water molecules and eight coordinated water ligands (calcd 8.47 %). The last weight loss of 6.61 % from 425 to 1000 ºC was corresponded to the removal of two $As_2O_3$, two ligands and the dehydration of the protons (calcd 6.57 %). The first weight loss is more than the theoretical value, which may be ascribed to the fact that the samples have been weathered before the thermogravimetric analyses. The thermogravimetric analyses of compounds **2Tb** and **3Dy** are shown in Table S3.

**Table S4.** Crystal Data and Structure Refinements for **1Eu**-**3Dy**.

| parameter | **1Eu** | **2Tb** | **3Dy** |
|---|---|---|---|
| Formula | $C_8H_{155}As_4Eu_6K_{11}O_{218}W_{38}$ | $C_8H_{123}As_4Tb_6K_{11}O_{202}W_{38}$ | $C_8H_{121}As_4Dy_6K_{15}O_{203}W_{38}$ |
| $M_r$ (g mol$^{-1}$) | 12367.66 | 12121.18 | 12313.01 |
| λ (Å) | 0.71073 | 0.71073 | 0.71073 |
| T [K] | 296(2) | 296(2) | 296(2) |
| crystal system | Triclinic | Triclinic | Triclinic |
| Space group | *P-1* | *P-1* | *P-1* |
| *a* (Å) | 12.627(2) | 15.320(2) | 19.5603(8) |
| *b* (Å) | 18.389(3) | 18.945(3) | 22.5308(9) |
| *c* (Å) | 23.142(4) | 19.928(3) | 26.0965(11) |
| *α* (deg) | 81.280(3) | 97.119(2) | 91.6410(10) |
| *β* (deg) | 80.406(3) | 99.267(2) | 100.0280(10) |
| *γ* (deg) | 80.720(3) | 102.633(3) | 108.4640(10) |
| *V* (Å$^3$) | 5185.9(16) | 5493.9(14) | 10699.0(8) |
| Z | 1 | 1 | 2 |
| $D_c$ (g cm$^{-3}$) | 3.789 | 3.531 | 3.716 |
| μ (mm$^{-1}$) | 23.719 | 22.600 | 23.405 |
| limiting indices | −15≤h≤14, −18≤k≤21, −27≤l≤26 | −18≤h≤13, −22≤k≤22, −23≤l≤23 | −23≤h≤23, −25≤k≤26, −31≤l≤22 |
| Params | 1207 | 1126 | 2276 |
| reflns collected | 26299 | 29057 | 56635 |
| $R_{int}$ | 0.0488 | 0.0459 | 0.0374 |
| GOF | 1.019 | 0.989 | 1.025 |
| $R_1$[a] [I >2σ (I)] | 0.0735 | 0.0747 | 0.0595 |
| $wR_2$[b] [I >2σ (I)] | 0.1851 | 0.1996 | 0.1620 |
| $R_1$[a] [all data] | 0.1200 | 0.0940 | 0.0775 |
| $wR_2$[b] [all data] | 0.2227 | 0.2208 | 0.1786 |
| Δ ρ $_{max}$/Δρ$_{min}$ (eÅ$^{-3}$) | 3.82/-2.55 | 3.41/-3.12 | 3.66/-1.93 |

[a] $R_1=\Sigma||F_o|-|F_c||/\Sigma|F_o|$. [b] $wR_2=\{\Sigma[w(F_o^2-F_c^2)^2]/\Sigma[w(F_o^2)^2]\}^{1/2}$.

**Table S5.** Selected bond distances of **1Eu**-**3Dy**.

| **1Eu** | | **2Td** | | **3Dy** | |
|---|---|---|---|---|---|
| Eu1—O1W | 2.41(2) | Tb1—O1W | 2.35(17) | Dy1—O149 | 2.42(13) |
| Eu1—O2W | 2.49(2) | Tb1—O2W | 2.42(16) | Dy1—O1W | 2.39(14) |
| Eu1—O34 | 2.40(19) | Tb1—O34 | 2.37(15) | Dy1—O2 | 2.27(13) |
| Eu1—O40 | 2.36(2) | Tb1—O40 | 2.34(18) | Dy1—O2W | 2.45(16) |
| Eu1—O42 | 2.47(2) | Tb1—O42 | 2.39(17) | Dy1—O33 | 2.31(14) |
| Eu1—O43 | 2.45(17) | Tb1—O51 | 2.23(17) | Dy1—O35 | 2.44(14) |
| Eu1—O66 | 2.33(2) | Tb1—O58 | 2.312(13) | Dy1—O3W | 2.45(16) |
| Eu1—O69 | 2.30(2) | Tb1—O43 | 2.28(15) | Dy1—O66 | 2.32(12) |
| Eu2—O10 | 2.58(18) | Tb2—O15 | 2.61(14) | Dy2—O149 | 2.39(13) |
| Eu2—O2 | 2.38(2) | Tb2—O23 | 2.30(16) | Dy2—O151 | 2.57(15) |
| Eu2—O3W | 2.42(2) | Tb2—O3W | 2.43(16) | Dy2—O30 | 2.34(13) |
| Eu2—O42 | 2.62(2) | Tb2—O42 | 2.57(14) | Dy2—O31 | 2.59(12) |
| Eu2—O43 | 2.43(2) | Tb2—O43 | 2.37(17) | Dy2—O33 | 2.36(14) |
| Eu2—O4W | 2.44(2) | Tb2—O4W | 2.46(15) | Dy2—O35 | 2.64(13) |
| Eu2—O58 | 2.39(19) | Tb2—O58 | 2.39(16) | Dy2—O41 | 2.30(12) |
| Eu2—O60 | 2.66(19) | Tb2—O60 | 2.56(17) | Dy2—O4W | 2.38(14) |
| Eu2—O66 | 2.43(18) | Tb2—O66 | 2.33(14) | Dy2—O5W | 2.45(16) |
| Eu3—O15 | 2.31(18) | Tb3—O15 | 2.47(16) | Dy3—O147 | 2.35(14) |
| Eu3—O43 | 2.43(2) | Tb3—O43 | 2.39(15) | Dy3—O149 | 2.43(12) |
| Eu3—O51 | 2.30(19) | Tb3—O5W | 2.40(16) | Dy3—O151 | 2.40(14) |
| Eu3—O58 | 2.36(16) | Tb3—O66 | 2.29(14) | Dy3—O23 | 2.23(13) |
| Eu3—O5W | 2.46(2) | Tb3—O69 | 2.27(18) | Dy3—O30 | 2.32(12) |
| Eu3—O6W | 2.462(2) | Tb3—O6W | 2.44(17) | Dy3—O67 | 2.34(12) |
| Eu3—O7W | 2.44 (3) | Tb3—O7W | 2.42(2) | Dy3—O6W | 2.41(15) |
| Eu3—O10 | 2.54(2) | Tb3—O8 | 2.32(16) | Dy3—O7W | 2.38(15) |
| As1—O18 | 1.83(19) | As1—O18 | 1.83(14) | As1—O18 | 1.79(14) |
| As1—O28 | 1.76(19) | As1—O28 | 1.79(17) | As1—O28 | 1.80(13) |
| As1—O6 | 1.76(17) | As1—O6 | 1.79(15) | As1—O6 | 1.82(12) |
| As2—O49 | 1.77(2) | As2—O49 | 1.78(18) | As2—O39 | 1.79(13) |
| As2—O61 | 1.78(19) | As2—O61 | 1.79(18) | As2—O51 | 1.81(13) |
| As2—O72 | 1.80(16) | As2—O72 | 1.76(15) | As2—O61 | 1.84(12) |
| W10—O24 | 1.88(16) | W10—O33 | 2.17(18) | W10—O34 | 1.74(14) |
| W10—O33 | 2.14(2) | W10—O34 | 1.72(17) | W10—O35 | 1.81(14) |
| W10—O34 | 1.73(19) | W10—O35 | 1.71(17) | W10—O36 | 1.91(15) |
| W10—O35 | 1.78(3) | W10—O36 | 2.14(15) | W10—O37 | 2.03(15) |
| W10—O36 | 2.18(2) | W10—O38 | 1.93(13) | W10—O38 | 1.93(13) |
| W10—O38 | 1.93(2) | W10—O4 | 1.89(14) | W10—O39 | 2.34(13) |